Materials Research. 2020; 23(2): e20190521
DOI: https://doi.org/10.1590/1980-5373-MR-2019-0521

Synthesis of Aurivillius Phase $CaBi_4Ti_4O_{15}$ Doped with both La^{3+} and Mn^{3+} Cations: Crystal Structure and Dielectric Properties

Zulhadjri Zulhadjri [a]*, Aulia Arivin Billah[a], Tio Putra Wendari[a], Emriadi Emriadi[a], Upita Septiani[a], Syukri Arief[a]

[a]*Universitas Andalas, Faculty of Mathematics and Natural Sciences, Department of Chemistry, Kampus Limau Manis, Padang 25163, Indonesia*

Received: September 16, 2019; Revised: February 17, 2020; Accepted: March 30, 2020

The four-layer Aurivillius $CaBi_4Ti_4O_{15}$ with introducing of La^{3+} on the *A*-site and Mn^{3+} on the *B*-site with the formula $Ca_{1-x}Bi_{3+x}LaTi_{4-x}Mn_xO_{15}$ ($x = 0$, 0.2, 0.4, 0.6, 0.8, and 1) were synthesized by molten salt method using the mixture of sulfate salts K_2SO_4/Na_2SO_4 as the flux. XRD data confirmed the formation of single-phase Aurivillius with $A2_1am$ orthorhombic structure for $x = 0$, 0.2, 0.4, and 0.6, whereas for $x = 0.8$ and 1, the impurity phases were observed. SEM analysis shows the anisotropic plate-like grains, which are a typical grain of Aurivillius phases. The cell volume decreases with increasing *x*, indicating a presence of mixed valences of Mn^{3+} and Mn^{4+}. The dielectric constants increased with *x*, strongly correlated with the higher distortion of the structure, since the $6s^2$ lone pair electrons of Bi^{3+} cation increase. The presence of Mn^{3+} unpaired electrons results in the increase of dielectric loss as increasing *x*.

Keywords: *Aurivillius phase, molten salts, orthorhombic structure, dielectric properties*

1. Introduction

Oxide compounds based on Aurivillius phase have received much attention in recent years due to their sufficiently good dielectric properties and high ferroelectric–paraelectric phase transition temperature, which can be applied as memory cells, capacitors, sensors, and high-temperature piezoelectric transducers, etc[1-3]. In general, the formula of Aurivillius phase can be described as $(Bi_2O_2)^{2+}(A_{m-1}B_mO_{3m+1})^{2-}$, where the *A* represents the mono-, di-, trivalent cations with dodecahedral coordination (e.g., Na^+, Ca^{2+}, Pb^{2+}, Ba^{2+}, Sr^{2+}, Ln^{3+}) and the *B* represents the transition metal cation with octahedral coordination, which is smaller than *A*-site cation (e.g., Ti^{4+}, Ta^{5+}, Nb^{5+}, W^{6+}). The structure is constructed by an ordered intergrowth of bismuth layers $[Bi_2O_2]^{2+}$ and *m* perovskite-like layers $[A_{m-1}B_mO_{3m+1}]^{2-}$[4].

Recently, the modification of Aurivillius properties by introducing a magnetic transition cation (d^n) into the *B*-site of perovskite layers have received much interest due to this may result in multiferroic properties, which exhibit the coupling of both ferroelectric and magnetic properties[5]. The introduction of the magnetic cation with different ionic radius leads to a higher degree of BO_6 distortion and hence the dielectric properties. Besides, the substitution of lanthanides (Ln^{3+}) for Bi^{3+} has been reported to improve the electrical properties of the Aurivillius phase[6,7]. Several magnetoelectric materials based on Aurivillius phase have been reported for formula $Pb_{1-2x}Bi_{1.5+2x}La_{0.5}Nb_{2-x}Mn_xO_9$, $Pb_{1-x}Bi_{4+x}Ti_{4-x}Mn_xO_{15}$, $Pb_{2-x}Bi_{4+x}Ti_{5-x}Mn_xO_{18}$, and exhibited the improvement in dielectric properties[8-10].

Four-layered Aurivillius phase with formula $CaBi_4Ti_4O_{15}$ (CBT) has a high Curie temperature (T_c) of ferroelectric around 790 °C[11]. It is interesting to modify CBT by doping with La^{3+} and Mn^{3+} cations simultaneously with formula $Ca_{1-x}Bi_{3+x}LaTi_{4-x}Mn_xO_{15}$ (CBLTM) to produce a magnetoelectric compound. Based on the nominal formula, the substitution of Mn^{3+} for Ti^{4+} at the *B*-site is adjusted by the substitution of Bi^{3+} for Ca^{2+} at the *A*-site to keep neutrality of charge in the compound. To the best of our knowledge, the synthesis of this formula has not previously been reported. We use the molten salt method since it was reported to have successfully synthesized the multiferroic Aurivillius phase[12,13]. In this paper, the synthesis, crystal structure, and dielectric properties of products were investigated.

2. Experimental

The raw materials of $CaCO_3$, Bi_2O_3, TiO_2, Mn_2O_3, La_2O_3 (Aldrich, ≥ 99.9%) were weighed stoichiometrically for the formula $Ca_{1-x}Bi_{3+x}LaTi_{4-x}Mn_xO_{15}$ ($x = 0$, 0.2, 0.4, 0.6, 0.8, and 1) and then ground together with the mixture of Na_2SO_4/K_2SO_4 salts (1:1 molar ratio) for 2 hours. The amount mixture of Na_2SO_4/K_2SO_4 (1:1 molar ratio) was added 1:7 molar ratio of salt to oxide. The mixtures powders were put into an alumina crucible and heated at 750 °C, 850 °C, and 900 °C for 5 h for each heating step. Finally, the alkali salts were removed by washing with hot distilled water for several times and the product then dried at 110 °C for 24 hours. The phase identification was performed by X-ray diffraction (Shimadzu XRD 7000) using Cu Kα radiation. The Le Bail refinement method by the RIETICA program was used to determine the cell parameters of samples. Morphology analysis was analyzed by scanning electron microscopy (SEM HITACHI S-3400). The density of the sample was measured by Archimedes method. For the dielectric measurement, the obtained powders were pressed into pellets with a

*e-mail: zulhadjri@sci.unand.ac.id

diameter of 1 cm and thickness 0.1 cm, then heated at 800 °C for 8 hours to form a ceramic. Silver conductive paste (Aldrich, 99%) was pasted on both surfaces as electrodes. The room temperature capacitance and loss were measured using LCR meter (Agilent 4980A) with an applied voltage of 1 V over the frequencies range of 1kHz to 1 MHz.

3. Results and Discussion

The results of X-ray diffraction (XRD) analysis of $Ca_{1-x}Bi_{3+x}LaTi_{4-x}Mn_xO_{15}$ (CBLTM) powders with $x = 0$, 0.2, 0.4, 0.6, 0.8, and 1 are given in Figure 1. All XRD patterns could be indexed using the $CaBi_4Ti_4O_{15}$ standard diffraction pattern with an orthorhombic structure and $A2_1am$ space group (ICSD-99500). The single-phase of four-layer Aurivillius were obtained for x = 0, 0.2. 0.4, and 0.6, whereas for $x = 0.8$ and 1, the samples contained impurities identified as $Bi_2La_2Ti_3O_{12}$ (ICSD-150091) and $Bi_2Mn_4O_{10}$ (ICSD-26806).

The single-phase sample of x = 0 confirmed the 25% molar ratio La^{3+} was successfully substituted in Bi^{3+} site of $CaBi_4Ti_4O_{15}$. Furthermore, the Ti^{4+} could be simultaneously substituted by Mn^{3+} up to 15% molar ratio Ti^{4+} with adjusted the Ca:Bi ratio as the nominal formula for $x = 0.6$. The substitution of Mn^{3+} on the *B*-site cation up to 15% molar ratio has been reported in our previous reports both for four-layer Aurivillius $Pb_{1-x}Bi_{4+x}Ti_{4-x}Mn_xO_{15}$ and double-layer Aurivillius $Pb_{1-2x}Bi_{1.5+2x}La_{0.5}Nb_{2-x}Mn_xO_9$ synthesized by the molten salt method[8,9]. The presence of impurities for x = 0.8 and 1 is suggested due to the oxidizing Mn^{3+} to Mn^{4+} in samples. It has been reported that molten salt fluxes tend to form oxidizing species in solution due to an oxygen donor mechanism involving basic SO_4^{2-} anions, as explained by Lux-Flood theory[14]. This phenomenon of mixed-valent Mn^{3+}/Mn^{4+} has also been observed in molten salt synthesis of Aurivillius phase under an oxygen-rich sintering atmosphere[9,15]. The formation of higher oxidation states Mn^{4+} with increasing x leads to the non-stoichiometric charges, which causes the instability of crystal structure. This is in agreement with the impurity found in samples $x = 0.8$ and 1, where $Bi_2Mn_4O_{10}$ contains the Mn^{4+} ions that do not construct the perovskite layers, thus breaks the interlayer structure forming the three-layer Aurivillius phase $Bi_2La_2Ti_3O_{12}$ as another impurity.

Furthermore, the strongest (119) diffraction peak corresponds well with the (112*m*+1) strongest diffraction peak in the four-layer Aurivillius phase, where $m = 4$ describes the number of layers. The crystallite size calculated using Scherrer's formula is approximately 48 nm, 66 nm, 61 nm, and 52 nm for $x = 0$, 0.2, 0.4, and 0.6, respectively. The results showed the tendency of an increase in the crystallinity of the samples containing Mn^{3+}.

Lattice parameters of the single-phase samples were evaluated by the Le Bail refinement in the RIETICA program using the structural parameter of $A2_1am$ $CaBi_4Ti_4O_{15}$ phase. The results of refinement fitting are shown in Figure 2. The good fits between the Le Bail plot of samples and the $A2_1am$ models demonstrate that the introduction of La^{3+} and Mn^{3+} cations does not change the parent structure. The refined lattice parameters and cell volume of single-phase $Ca_{1-x}Bi_{3+x}LaTi_{4-x}Mn_xO_{15}$ were shown in Figure 3.

The *a* and *b* lattice parameters are relatively constant, while the *c* lattice parameters tend to decrease as *x* increase. Since the ionic radius of Bi^{3+} (1.31 Å) in 12-fold coordination is similar to Ca^{2+} (1.34 Å) and the ionic radius of Ti^{4+} (0.605 Å) in 6-fold coordination similar to Mn^{3+} (0.645 Å)[16,17], the cell volume should not exhibit the significant difference with increasing *x*. However, it is observed that the cell volume decreases with increasing *x*. This might occur due to the smaller ionic radius of Mn^{4+} (0.54 Å) than that of Mn^{3+}

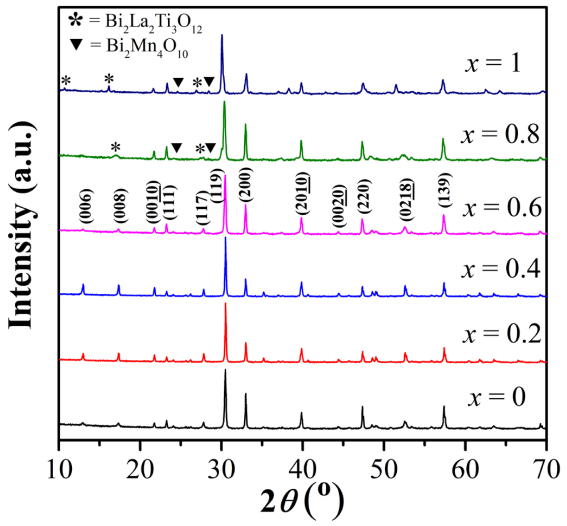

Figure 1. Powder X-ray diffraction patterns of $Ca_{1-x}Bi_{3+x}LaTi_{4-x}Mn_xO_{15}$ samples were synthesized by molten salt method. The $x = 0.8$ and 1.0 samples indicate peaks from the impurity $Bi_2La_2Ti_3O_{12}$ and $Bi_2Mn_4O_{10}$ phase.

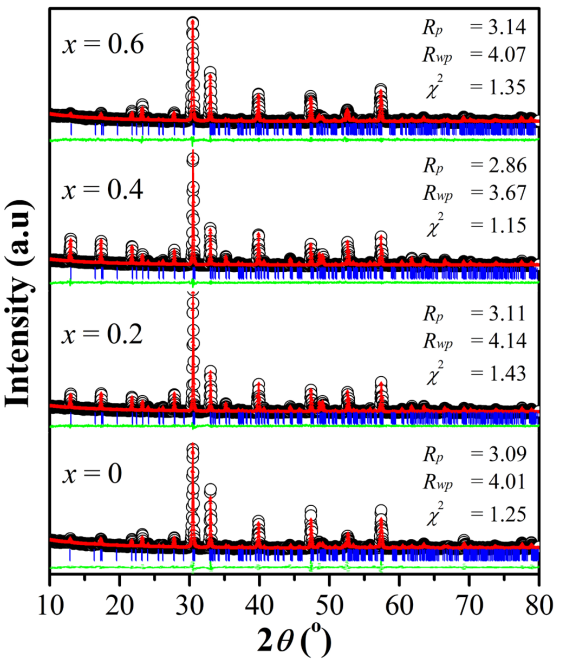

Figure 2. Le Bail plot of XRD powder of $Ca_{1-x}Bi_{3+x}LaTi_{4-x}Mn_xO_{15}$ with $x = 0$, 0.2, 0.4, and 0.6. Observed XRD intensity (circle), calculated data (solid line), and the difference of patterns, y_{obs}-y_{cal} (solid line on the bottom curve). The tick marks represent the positions of allowed Bragg reflections in the phase of $A2_1am$.

(0.645 Å) in 6-fold coordination. The formation of Mn^{4+} ions on the *B*-site can also be observed by the decrease of *c* lattice parameter, which corresponds to the shrinkage of the BO_6 octahedra[18]. The presence of mixed-valent Mn^{3+}/Mn^{4+} with increasing *x* confirmed the suggestion of possible impurity phases, as evidenced by the XRD discussion above.

The density of single-phase samples increase slightly with increasing *x* was about 6.49 g/cm^3, 6.66 g/cm^3, 6.84 g/cm^3, and 6.95 g/cm^3 for $x = 0$, 0.2, 0.4, and 0.6, respectively. This increased density was also obtained from the refinement result. The relative density was calculated according to the experimental density and theoretical density. The relative density of single-phase samples is higher than 93% of theoretical density, indicating a well-densified grain can be achieved by the molten salt method.

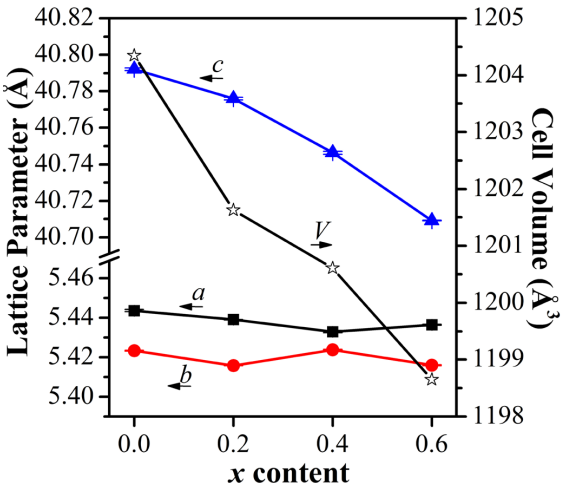

Figure 3. Lattice parameters and cell volume of single-phase $Ca_{1-x}Bi_{3+x}LaTi_{4-x}Mn_xO_{15}$ obtained from XRD refinement results.

The powder morphology of single-phase samples analyzed by SEM is shown in Figure 4. Anisotropic plate-like grains, a typical grain for layered compounds belonging to the Aurivillius phase was observed for all samples. The average grain size is in the range 0.6 - 2.7 µm for $x = 0$, 1.2 – 6.3 µm for $x = 0.2$, 0.9 - 4.3 µm for $x = 0.4$, and 0.9 – 3.3 µm for $x = 0.6$. The results showed the same tendency with the crystallite size, where the larger grain size obtained in the samples containing Mn^{3+}.

The frequency dependence of the dielectric constant and dielectric loss of single-phase samples measured at room temperature is shown in Figure 5. All samples showed a strong dielectric dispersion at low frequency and becomes stable at the high frequency of 100 kHz, which is typical behavior for the common ferroelectric phase. This behavior is due to the different types of polarization (i.e. dipolar, ionic, electronic, and interfacial) and the accumulation of charge carriers on the surface and at grain boundaries, known as the Maxwell-Wagner effect[5,19]. Therefore, we focus on the dielectric properties of samples at higher frequencies since it properly exhibits the intrinsic polarizability of samples.

The dielectric constant value at 100 kHz increases as *x* increases, where the value is 206.03, 342.4, 491.11, and 868.41 for $x = 0$, 0.2, 0.4, and 0.6, respectively. It was reported that the presence of *A*-site cations with $6s^2$ lone

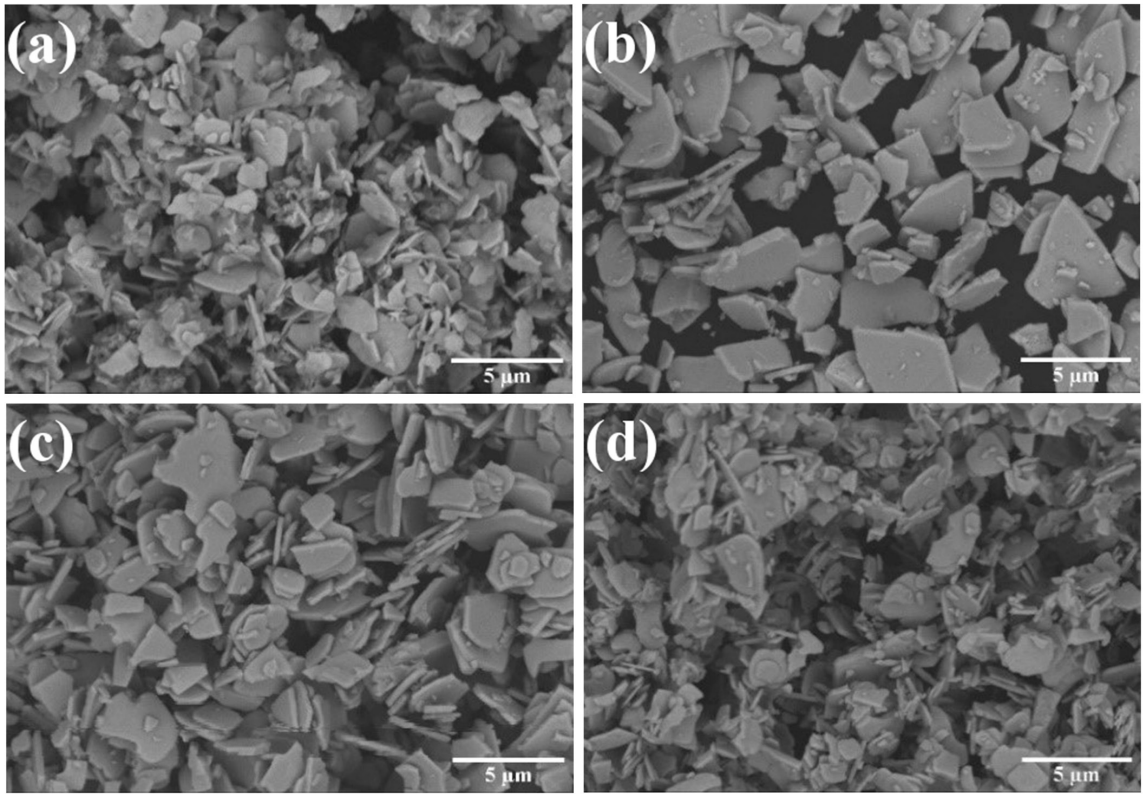

Figure 4. SEM micrographs of the single-phase $Ca_{1-x}Bi_{3+x}LaTi_{4-x}Mn_xO_{15}$ powder. (a) $x = 0$ (b) $x = 0.2$ (c) $x = 0.4$, and (d) $x = 0.6$.

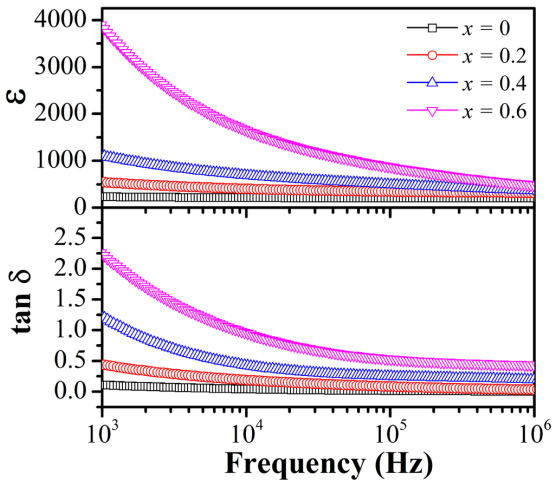

Figure 5. Frequency dependence of dielectric constant (ε) and loss (tan δ) of single-phase $Ca_{1-x}Bi_{3+x}LaTi_{4-x}Mn_xO_{15}$ at room temperature.

pair electrons such as Bi^{3+} strongly favors a highly distorted structure, resulting in increased polarization[8,20]. According to the nominal formula, the substitution of Mn^{3+} for Ti^{4+} on the *B*-site was compensated by the increasing proportion of Bi^{3+} cations, which could result in the higher distortion of BO_6 octahedra. Furthermore, the occupancy of cations with different radii caused the mismatch between bismuth and perovskite layers, which also gives rise to the highly distorted structure. Therefore, both factors contribute to the ferroelectric displacement and further hence a higher magnitude of dielectric constant.

The high dielectric loss (tan δ) is found at the lower frequency is due to the interfacial polarization between electrode and sample. Furthermore, the tan δ values of single-phase samples increase with increasing *x* with value 0.0166 for $x = 0$ to 0.0834 for $x = 0.2$, 0.2473 for $x = 0.4$, and 0.5291 for $x = 0.6$ at 100 kHz. The substitution of Mn^{3+} for Ti^{4+} increase in the unpaired electron concentrations as the charge carriers, which results in the higher electrical conductivity[8]. Besides, the formation of the mixed-valent Mn^{3+} and Mn^{4+} in the higher *x*, as discussed in the refinement results above, probably induced the electron transport via Mn^{3+}-O-Mn^{4+} double-exchange interaction contributing to a significant increase in dielectric loss value of $x = 0.4$ and 0.6 samples.

4. Conclusion

The single phases of four-layer Aurivillius compound $Ca_{1-x}Bi_{3+x}LaTi_{4-x}Mn_xO_{15}$ ($x = 0$, 0.2, 0.4, and 0.6) have been successfully synthesized by the molten salt method. All samples showed an orthorhombic crystal structure with the $A2_1am$ space group. The results confirmed that La^{3+} successfully substituted for Bi^{3+} and simultaneously substituted Mn^{3+} for Ti^{4+}. The cell volume as the lattice parameter *c* decrease with increasing *x*, which attributed to the formation of smaller Mn^{4+} cations on *B*-site. The dielectric constant increases with increasing *x*, which is correlated to the increases structural distortion induced by the increasing Bi^{3+} composition The increased concentration of Mn^{3+} unpaired electrons as charge carriers exhibits a higher dielectric loss, indicating the sample more conductive.

5. Acknowledgment

The authors thank the Ministry of Research, Technology and Higher Education of Indonesia and LPPM of Andalas University for financial support for this work through the Fundamental Grant with contract number 051/SP2H/LT/DRPM/2019.

6. References

1. Whatmore R. Ferroelectric materials. In: Kasap S, Capper P. Springer handbook of electronic and photonic materials. Cham: Springer; 2017. p. 589-614.
2. Chen A. A review of emerging non-volatile memory (NVM) technologies and applications. Solid-State Electron. 2016;125:25-38.
3. Guo R, You L, Zhou Y, Lim ZS, Zou X, Chen L, et al. Non-volatile memory based on the ferroelectric. Nat Commun. 2013;4:2-6.
4. Aurivillius B. Mixed bismuth oxides with layer lattices 1. The structure type of $CaNb_2Bi_2O_9$. Ark Kemi. 1949;1:463-80.
5. Xiao J, Zhang H, Xue Y, Lu Z, Chen X, Su P, et al. The influence of Ni-doping concentration on multiferroic behaviors in $Bi_4NdTi_3FeO_{15}$ ceramics. Ceram Int. 2015;41(1):1087-92.
6. Nayak P, Badapanda T, Panigrahi S. Dielectric and ferroelectric properties of Lanthanum modified $SrBi_4Ti_4O_{15}$ ceramics. Mater Lett. 2016;172:32-5.
7. Diao C, Li H, Chen Z, Zheng H. Effect of samarium substitution on the dielectric and ferroelectric properties of $BaBi_{4-x}Sm_xTi_4O_{15}$ ceramics. Ceram Int. 2016;42(1):621-6.
8. Wendari TP, Arief S, Mufti N, Suendo V, Prasetyo A, Ismunandar, et al. Synthesis, structural analysis and dielectric properties of the double-layer Aurivillius compound $Pb_{1-2x}Bi_{1.5+2x}La_{0.5}Nb_{2-x}Mn_xO_9$. Ceram Int. 2019;45(14):17276-82.
9. Zulhadjri, Prijamboedi B, Nugroho AA, Mufti N, Fajar A, Palstra TTM, et al. Aurivillius phases of $PbBi_4Ti_4O_{15}$ doped with Mn^{3+} synthesized by molten salt technique: structure, dielectric, and magnetic properties. J Solid State Chem. 2011;184:1318-23.
10. Zulhadjri, Prijamboedi B, Nugroho AA, Mufti N. Ismunandar. Five layers aurivillius phases $Pb_{2-x}Bi_{4+x}Ti_{5-x}Mn_xO_{18}$: synthesis, structure, relaxor ferroelectric and magnetic properties. ITB J Sci. 2011;43(2):139-50.
11. Sheng L, Du X, Chao Q, Zheng P, Bai W, Li L, et al. Enhanced electrical properties in Nd and Ce co-doped $CaBi_4Ti_4O_{15}$ high temperature piezoceramics. Ceram Int. 2018;44(15):18316-21.
12. Chen X, Lu Z, Huang F, Min J, Li J, Xiao J, et al. Molten salt synthesis and magnetic anisotropy of multiferroic $Bi_4NdTi_3Fe_{0.7}Ni_{0.3}O_{15}$ ceramics. J Alloys Compd. 2017;693:448-53.
13. Fuentes L, García M, Bueno D, Fuentes ME, Muñoz A. Ferroelectrics magnetoelectric effect in $Bi_5Ti_3FeO_{15}$ ceramics obtained by molten salts synthesis. Ferroelectrics. 2006;336:81-9.
14. Boltersdorf J, King N, Maggard PA. Flux-mediated crystal growth of metal oxides: synthetic tunability of particle morphologies, sizes, and surface features for photocatalysis research. CrystEngComm. 2015;17(11):2225-41.
15. Wendari TP, Arief S, Mufti N, Insani A, Baas J, Blake GR, et al. Structural and multiferroic properties in double-layer Aurivillius phase $Pb_{0.4}Bi_{2.1}La_{0.5}Nb_{1.7}Mn_{0.3}O_9$ prepared by molten salt method. J Alloys Compd. 2020;820:153145.
16. Tellier J, Boullay P, Manier M, Mercurio D. A comparative study of the Aurivillius phase ferroelectrics $CaBi_4Ti_4O_{15}$ and $BaBi_4Ti_4O_{15}$. J Solid State Chem. 2004;177:1829-37.

17. Shannon RD. Revised effective ionic radii and systematic studies of interatomie distances in halides and chaleogenides. Acta Crystallogr. 1976;32:751-67.
18. Yu Z, Yu B, Liu Y, Zhou P, Jiang J, Liang K, et al. Enhancement of multiferroic properties of Aurivillius $Bi_5Ti_3FeO_{15}$ceramics by Co doping. Ceram Int. 2017;43(17):14996-5001.
19. Mohapatra A, Das PR, Choudhary RNP. Structural and electrical properties of La modified $Bi_5Ti_3FeO_{15}$ ceramics. J Mater Sci Mater Electron. 2015;26(5):3035-43.
20. Chang Q, Fan H, Long C. Effect of isovalent lanthanide cations compensation for volatilized A-site bismuth in Aurivillius ferroelectric bismuth titanate. J Mater Sci Mater Electron. 2017;28(6):4637-46.